Sensitivity investigation of backgated silicon nanowire biosensors for liquid gatting

By

MD. Jakaria Yusuf Khan

(ID: 2011-1-80-039)

And

Md. Shafquatur Rahman

(ID: 2011-1-80-059)

And

Mehedi Hasan

(ID: 2011-1-80-061)

Submitted to the

Department of Electrical & Electronics Engineering, Faculty of Science and Engineering

East West University

In partial fulfillment of the requirements for the degree of Bachelor of Science in Electrical & Electronics Engineering

(B.Sc. in EEE)

Summer, 2015

Approved By

Academic Advisor	Department Chairperson
Dr. Mohammad Mojammel AL Hakim	Dr. Halima Begum

Approval

The thesis title “An investigation on the accumulation mode Si-NW transistors’ sub-threshold characteristics modulation using backgate bias at different NW lengths and NW thicknesses” submitted by Md. Jakaria Yusuf Khan [2011-1-80-039], Md. Shafquatur Rahman [2011-1-80-059] and Mehedi Hasan [2011-1-80-061] in the semester of summer-2015 is approved satisfactory in partial fulfillment of the requirements for the requirements for the degree of Bachelor of Science in Electrical and Electronics Engineering.

Dr. Mohammad Mojammel AL Hakim

Associate Professor, Department of Electrical and Electronics Engineering

East West University, Dhaka, Bangladesh

Declaration

We, hereby declare that this material which we now submit for assessment on the program of study leading to the award of Bachelor's Degree in Electrical and Electronics Engineering is entirely our own work and we have exercised reasonable care to ensure that the work is original and does not to the best of our knowledge breach any law of copyright, and has not been taken from the work of others. Any reference from outside source has been cited and acknowledged within the text of our work.

_____

Md. Jakaria Yusuf Khan

_____

Md. Shafquatur Rahman

_____

Mehedi Hasan

Summer Semester

August’ 2015

Abstract

We performed a feasibility study of tailoring sensitivity of Si nanowire through backgate bias arrangement for various NW length and thickness. Three different thicknesses of 100 nm, 50 nm and 25 nm were chosen and each thickness consisted of 5 different channel lengths - 1000 nm, 750 nm, 500 nm, 250 nm and 100 nm respectively. It can be seen that the backgate bias has a big influence on the sensitivity of a p-type SiNW. A backgate bias leading to a depletion of the NW body increases the sensitivity whereas the backgate bias leading to an accumulation of significant carriers decreases the sensitivity of NW. For a fixed NW thickness, a decrease of NW length found to degrade sub-threshold slope and hence NW sensitivity. But for a fixed NW length a decrease of NW thickness improves the sub-threshold characteristics and sensitivity. When the NW thickness is 100 nm a peak sensitivity of 2390%/v is found for 1um long NW which degrades to a value of 349%/V at 100nm length. However, 100 nm long NW's sensitivity can be improved by reducing NW thickness and adjusting backgate bias. A 100 nm long 25 nm thick NW exhibits an improved sensitivity of 2730%/V with +7V of backgate bias. This result implies that with appropriate backgate bias arrangement, low doped then NW can be used for single molecule detection as biosensors. Our simulation revealed that a 25 nm thick 1 um long NW with +7V of backgate bias gives a sensitivity of 3050 %/V.

Acknowledgement

We would like to express our sincere gratitude to East West University for letting us fulfill our dream of becoming a student here. Our professor and supervisor Dr Muhammad Mujammel Al Hakim (a pioneer in the field of Nanotechnology) has been an immense help throughout our course of research. He provided us with his vast and profound knowledge on Biosensors and without his guidance and encouragement we could not have finished this project. Our gratitude also goes out to our families and friends for helping us survive through all the stress and not letting us give up on our dreams. Finally, thanks to The Almighty for giving us the patience required to finish this task successfully.

Authorization Page

We hereby certify that we are the sole authors of this thesis. We declare that the East West University shall have the rights to preserve, use and disseminate this dissertation/thesis in print or electronic format for academic/research purpose only after one year of submission.

_____

Md. Jakaria Yusuf Khan

_____

Md. Shafquatur Rahman

_____

Mehedi Hasan

We authorize East West University to produce this thesis by photocopy or other means, in total or in part, at the request of other institutions or individuals for the purpose of scholarly research only after one year of submission.

_____

_____

_____

Table of Content

Page Number

List of Figures

Page Number

List of Tables

Page number

CHAPTER 1: INTRODUCTION

1.1 Objective

Silicon nanowire field-effect transistors (SiNW-FETs) have recently drawn tremendous attention as a promising tool in biosensor design because of their ultrasensitivity, selectivity, and label-free and real-time detection capabilities. SiNW-FETs can be delicately designed to be a reusable device via a reversible surface functionalization method. In the fields of biological research, SiNW-FETs are employed in the detections of proteins, DNA sequences, small molecules, cancer biomarkers, and viruses[1].

With the rapid growth and development of advanced nanotechnology, many nanomaterials used for sensing with unique properties, desired size, and chemical compositions have been fabricated to be incorporated within the transducer. Of all the applications, one of them is the one-dimensional (1D) nanostructures which includes nanotubes, nanowires, nanorods, nanobelts and heteronanowires

Silicon nanowire is one of the 1D nanostructures and has emerged as the promising sensing nanomaterial with its unique mechanical, electronical, and optical properties. The fundamental cause as to why SiNWs have attracted attention in the development of ultrasensitive sensors is due to their high surface to volume ratios which greatly enhances the detection limit to fM concentrations and giving high sensitivity. Moreover, the dimension of SiNW is in the range of ≈1–100 nm, hence making it very comparable and compatible to the dimensional scale of biological and chemical species we want to investigate. Having the smallest dimension, SiNWs exhibited good electron transfer in detection because the accumulation of charge in SiNWs directly occurs within the bulk of material resulting in fast response of detection.

SiNWS are traditionally formed on SOI wafers in top down approaches and its burried Si layer could easily be used as an additional gate which may affect SiNW'S sensitivity as biosensor. In this work we first time perform a systemetic study on the effect of backgate bias on the sensitivity of P-Type Si NWS. Three different thicknesses of 100 nm, 50 nm and 25 nm were chosen and each thickness consisted of 5 different channel lengths of 1000 nm, 750 nm, 500 nm, 250 nm and 100 nm P-Type SiNW with a nominal doping of $10^{17}/cm^3$ has been investigated for different backgate biases and different drain bias polarities to gain insight into NW'S sensitivity through backgate bias arrangements.

1.2 Background

The conductance changes of silicon nanowires upon attachment of bimolecular have been employed extensively for bio sensing applications. Quite a number of works [2-5] can be founded in the literature exploiting this behavior for biosensors. However inherent nanowires

electrical characteristics are found to be quite variable although they have been successfully applied for bio sensing application. These are discussed below.

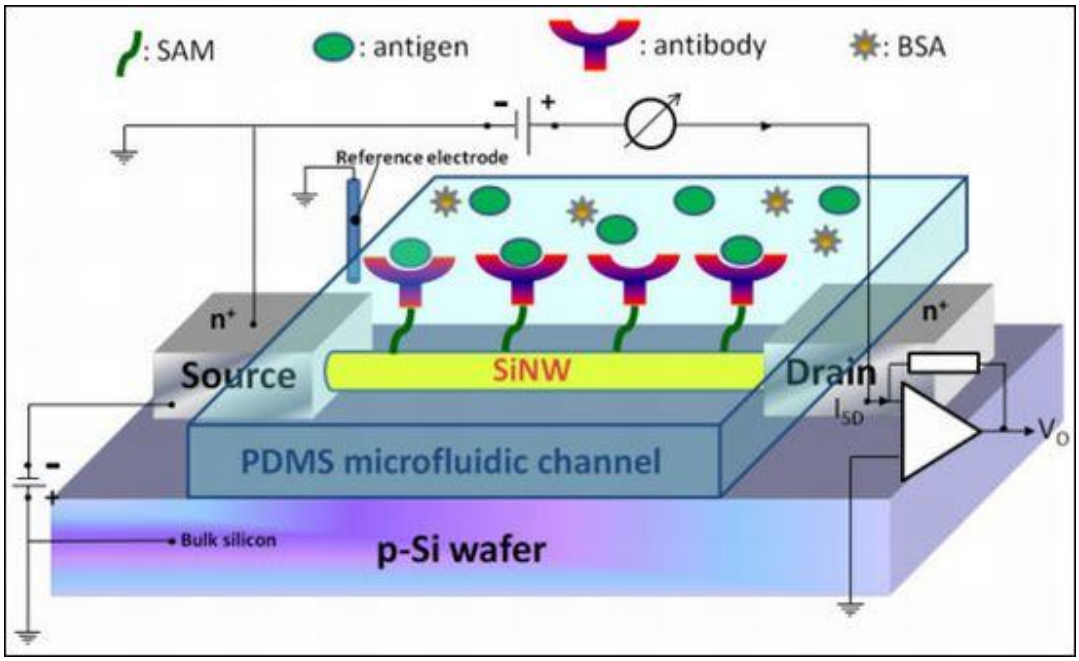

Figure 1.1: Schematic diagram of the structure of Si-nanowire biosensor.

A typical nanowire biosensor can be a single or an array of nanowires which is laid on an insulator between source and drain [Figure. 2.1]. Electrodes of these source and drain are isolated by a protection layer. On Si-nanowire surface, target receptors which have the capability of immobilizing the targets, e.g. ions, DNA, proteins are attached by molecular linkers. Due to large surface to volume ratio, the charges associated with the attached molecules can be deplete or accumulate entire cross sectional pathway. And hence nanowire conductance gets easily changed. This phenomenon resulted in the most promising breakthrough in the 21st century by possible application of simple nanowire device for disease diagnosis [6-12, 11-13].

Lieber et al. [2] successfully fabricated silicon nanowire biosensors on p-type semiconductor where the typical DC current voltage (I-V) characteristics were linear. The ability of the fabricated biosensors was tested through pH response with or without modifying nanowire surface containing both amino or silanol receptor. It was shown that increase of the solution pH level resulted in the increase of nanowire conductance due to the reduction of the protons in the solution and vice versa with typical sensitivity around 10% to 20% only. Real time detection of clinically relevant protein streptavidin was demonstrated down to concentrations of 10pM. Single DNA and wild type virus the DF508 also detected. This electrical detection was done to

concentration of 60fM. These results exhibited the promise of silicon nanowires as biosensor where nanowire's inherent DC characteristics were linear demonstrated general concept of nanowires just as simple constricted dimension resistors.

Chen et al. [3] fabricated p-type silicon nanowires using anew size reduction method where silicon nanowires have height of 140nm, width of 100nm with triangular structure and a uniform doping concentration of $N_a=10^{17}$ cm^{-3}. Measured current voltage (I-V) characteristics exhibited typically non-linear diode like characteristics. According to provided I-V curves there were no conduction up to a drain bias of $V_{ds}<1V$. The conduction of nanowires were improved through the application of negative back gate bias thereby increasing the accumulation of holes and at $V_{backgate}$ = -20Vthe I-V characteristics showed linear behavior. It was noticeable that at small negative $V_{backgate}$ I-V characteristics were typically nonlinear. This was attributed to the fixed electronic charge located in the front oxide near the top silicon device layer surface and buried oxide near the bottom of silicon device layer due to reactive thermal oxidation of silicon surface. These nanowires were also successfully sensed pH level of the solution with sensitivity around 40mV/pH

Most recently, Jean-Pierre Colinge et al. [4] first time reported that Si-Nanowires with a a few tens of nanometers wide, thickness of 20nm and uniform doping concentrations around 10^{19} cm^{-3}, behave as transistor than simple resistor. Both p-type and n-type silicon nanowires were fabricated and measured characteristics showed that both n-type and p-type devices exhibited transistor action. These devices showed near ideal sub-threshold slope of 64mv dec^{-1} and quite decent output characteristics.

The aforementioned survey shows that quite a variable electrical characteristic has been observed in the fabricated NW biosensors and sensitivity was controlled by arbitrary application of biased voltages. As Si NW sensitivity may depend on NW length, thickness and doping, sensitivity somehow remains fixed after fabrication for any fixed applied bias and surface chemistry. SOI platform has an unique opportunity to use backgate as an additional tuning method to improve sensitivity of NW. In this work we first investigated the intricate relationship of NW sensitivity with NW length and thicknesses. The possibility of tuning the sensitivity using backgate biases. Three different thicknesses of 100 nm, 50 nm and 25 nm were chosen and each thickness consisted of 5 different channel lengths - 1000 nm, 750 nm, 500 nm, 250 nm and 100 nm respectively. It can be seen that the backgate bias has a big influence on the sensitivity of a p-type SiNW. For a fixed NW thickness, a decrease of NW length found to degrade sub-threshold slope and hence NW sensitivity. But for a fixed NW length a decrease of NW thickness improves the sub-threshold characteristics and sensitivity. Our simulation revealed that a 25 nm thick 1 um long NW with +7V of backgate bias gives a sensitivity of 3050 %/V.

1.3 Organization

Chapter 1 provides the necessary background work on the electrical characteristics of silicon nanowires. A number of research paper on Si-NW biosensor have alsp been surveyed to gain an understanding on the importance of this work.

Chapter 2 describes device structure, simulation methodology and the required models for the simulation.

Chapter 3 describes the simulation results for nanowire thickness of 100nm, 50nm, 25nm and different nanowire length with doping concentration 10^{-16} cm^{-3} for different backgate bias condition.

Finally, in chapter 4 and 5, the contribution of this work is summarized and discussed.

CHAPTER 2: METHODOLOGY

2.1 Device features and simulation models

The investigation of sensitivity of Silicon nanowire for biosensor application were done with the help of numerical simulations using the SILVACO Atlas device simulator [14], installed on a VLSI lab of East West University. A p-type silicon nanowire with 100 nm, 50nm and 25nm thickness was created on 100 nm oxide with a 500 nm buried Si layer. 1000nm, 750nm, 500nm, 250nm, 100nm nanowire length are used for all those thickness. A secondary gate (backgate) is made with 20 nm Al beneath the buried Si layer. The gate oxide thickness was 2nm and a heavily doped poly-silicon layer was used as top gate material. In the silicon nanowire, two heavily doped regions on the two sides of the channel were employed to ensure ohmic contacts on the source/drain regions. The gate doping was $10^{20}/cm^3$ and the source/drain regions were also heavily doped with the doping density of $10^{20}/cm^3$. The channel doping was $10^{17}/cm^3$. Here, the gate doping was n-type whereas the drain and the channel doping was p-type. To contact source to drain and gate, aluminum electrode was chosen.

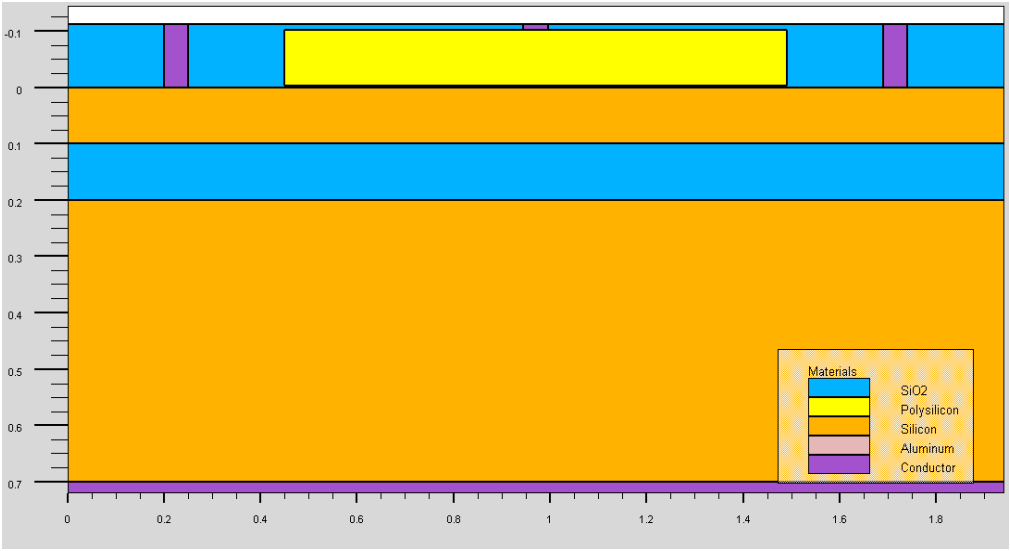

Figure 2.1: Schematic of the simulated p-type silicon nanowire.

As Si NW is 100nm, 50nm and 25nm thick quantum effect is neglected and a classical drift diffusion model is used to investigate SiNW behavior. To accurately model carrier mobility in the constructed volume of NW Lombardi (CVT) model was used to take account temperature (T_L), perpendicular electric field ($E_\perp$), parallel electric field ($E_\parallel$) and doping concentration (N) effects [3]. In the CVT model, the transverse field, doping dependent and temperature dependent parts of the mobility are given by the three components that are combined using Mathiessen's rule. These components are surface mobility limited by scattering with acoustic phonons (μ_{AC}), the mobility limited by surface roughness (μ_{sr}) and the mobility limited by scattering with optical intervalley phonons (μ_b) are combined using Mathiessen's rule as follows [14]

$$\mu_T^{-1} = \mu_{AC}^{-1} + \mu_b^{-1} + \mu_{sr}^{-1} \quad (2.1)$$

The first component, surface mobility limited by scattering with acoustic phonons equations [14]:

$$\mu_{AC.n} = \frac{BN.CVT}{E_\perp} + \frac{CN.CVT N^{\tau.CVT}}{T_L E_\perp^{\frac{1}{3}}} \quad (2.2)$$

$$\mu_{AC.p} = \frac{BN.CVT}{E_\perp} + \frac{CP.CVT N^{\tau P.CVT}}{T_L E_\perp^{\frac{1}{3}}} \quad (2.3)$$

The equation parameters BN.CVT, BP.CVT, CN.CVT, CP.CVT, TAUN.CVT, and TAUP.CVT used for this simulation are shown in Table 3-1 [15].

The second component, μ_{sr} is the surface roughness factor and is given by [14]:

$$\mu_{sr} = \frac{DELN.CVT}{E_\perp^2} \quad (2.4)$$

$$\mu_{sr} = \frac{DELP.CVT}{E_\perp^2} \quad (2.5)$$

The equation parameters DELN.CVT and DELP.CVT used for this simulation are shown in Table 3.1[14].

The third mobility component, the mobility limited by scattering with optical intervalley phonons is given by [14]:

$$\mu_{b,n} = MU0N.CVT exp\left(\frac{-PCN.CVT}{N}\right) + \frac{\left[MUMAXN.CVT\left(\frac{T_L}{300}\right)^{-GAMN.CVT} - MU0N.CVT\right]}{1+\left(\frac{N}{CRN.CVT}\right)^{ALPHN.CVT}} - \frac{MU1N.CVT}{1+\left(\frac{CSN.CVT}{N}\right)^{BETAN.CVT}} \quad (2.6)$$

$$\mu_{b,p} = MU0P.CVT exp\left(\frac{-PCP.CVT}{N}\right) + \frac{\left[MUMAXP.CVT\left(\frac{T_L}{300}\right)^{-GAMP.CVT} - MU0P.CVT\right]}{1+\left(\frac{N}{CRP.CVT}\right)^{ALPHP.CVT}} - \frac{MU1P.CVT}{1+\left(\frac{CSP.CVT}{N}\right)^{BETAP.CVT}} \quad (2.7)$$

Table 2.1: Parameters for Equations 2.1 to 2.7

Statement	Parameter	Default	Units
MOBILITY	BN.CVT	4.75×10^{7}	cm/(a)
MOBILITY	BP.CVT	9.925×10^{4}	cm/(a)
MOBILITY	CN.CVT	1.74×10^{5}	
MOBILITY	CP.CVT	8.842×10^{5}	
MOBILITY	TAUN.CVT	0.125	
MOBILITY	TAUP.CVT	0.0317	
MOBILITY	GAMN.CVT	2.5	
MOBILITY	GAMP.CVT	2.2	
MOBILITY	MU0N.CVT	52.2	cm^2/(v-a)
MOBILITY	MU0P.CVT	44.9	cm^2/(v-a)
MOBILITY	MU1N.CVT	43.4	cm^2/(v-a)
MOBILITY	MU1P.CVT	29.0	cm^2/(v-a)
MOBILITY	MUMAXN.CVT	1417.0	cm^2/(v-a)
MOBILITY	MUMAXP.CVT	470.5	cm^2/(v-a)
MOBILITY	CRN.CVT	9.68×10^{14}	cm^{-3}
MOBILITY	CRP.CVT	2.23×10^{17}	cm^{-3}
MOBILITY	CSN.CVT	3.43×10^{20}	cm^{-3}
MOBILITY	CSP.CVT	6.10×10^{20}	cm^{-3}
MOBILITY	ALPHN.CVT	0.680	
MOBILITY	ALPHP.CVT	0.71	
MOBILITY	BETAN.CVT	2.00	
MOBILITY	BETAP.CVT	2.00	
MOBILITY	PCN.CVT	0.0	cm^{-3}
MOBILITY	PCP.CVT	0.23×10^{16}	cm^{-3}
MOBILITY	DELN.CVT	5.82×10^{14}	v/s
MOBILITY	DELP.CVT	2.054×10^{14}	v^2/s

The model for carrier emission and absorption processes proposed by Shockley-Read-Hall (SRH) is used to reflect the recombination phenomenon within the device. The electron and hole lifetimes $\tau_{n\ and}\ \tau_p$were modeled as concentration dependent. The equation is given by [14]:

$$R_{SRH} = \frac{pn - n_{ie}^2}{\tau_p\left[n + n_{ie}exp\left(\frac{ETRAP}{kT_L}\right)\right] + \tau_n\left[p + n_{ie}exp\left(\frac{-ETRAP}{kT_L}\right)\right]} \quad (2.8)$$

$$\tau_n = \frac{TAUNO}{1 + \frac{N}{(NSRHN)}} \quad (2.9)$$

$$\tau_p = \frac{TAUPO}{1+\frac{N}{(NSRHP)}} \quad (2.10)$$

Here N is called the local (total) impurity concentration. The used parameters TAUN0, TAUP0, NSRHN and NSRHP are Table 3-2[14]. This model was activated with the CONSRH parameter of the MODELS statement.

Table 2.2: Default Parameters for Equations 2.8 to 2.10

Statement	Parameter	Default	Units
MATERIAL	TAUNO	1.0×10^{-7}	S
MATERIAL	NSRHN	5.0×10^{16}	cm^{-3}
MATERIAL	TAUPO	1.0×10^{-7}	S
MATERIAL	NSRHP	5.0×10^{16}	cm^{-3}

To account bandgap narrowing effects, BGN model was used. These effects may be described by an analytic expression relating the variation in bandgap, ΔE_g,to the doping concentration N. The expression used in ATLAS is from Slotboom and de Graaf [14]:

The used values for the parameters BGN.E, BGN.N and BGN.C are shown in Table 2.3[14].

Table 2.3: Default parameters of Slotbooms Bandgap Narrowing Model foe equation 2.11

Statement	Parameter	Default	Units
MATERIAL	BGN.E	9.0×10^{16}	V
MATERIAL	BGN.N	1.0×10^{16}	cm^{-3}
MATERIAL	BGN.C	0.5	-

2.2 Simulation profile

Device simulation using silvaco atlas usually faces convergence problems and necessitates a long run times. To avoid these problems, the simulation of silicon nanowire MOSFET has been divided into a few groups. At first, structure definition was performed. In this definition the simulation focused on creating the structure with a suitable mesh density. Regions and electrodes were defined as depicted in Fig. 2.2. Finer nodes were assigned in critical areas, such as across the gate oxide for an accurate 10nm thickness to monitor channel activity and to get a better picture of the depletion layer and junction behavior near the source/drain boundaries. A coarser mesh was used elsewhere in order to reduce simulation run time.

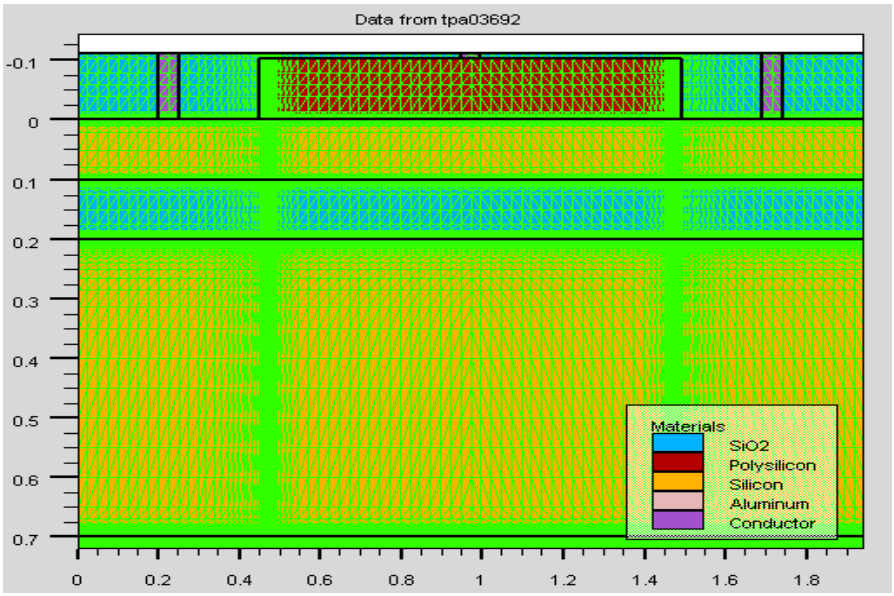

Figure 2.2: Cross-sectional view of p-type nanowire showing the mesh density used in this simulation.

Once the structure and the mesh were found to be as desired, the simulation was performed with appropriate models as discussed in section 3.1 and numerical solving methods. The model was invoked by using the statements FERMI, CVT, CONSRH, BGN. The numerical solving methods GUMMEL, NEWTON were used to reduce the simulation run time, while keeping the accuracy of the simulation at an acceptable level.

To get convergence, a special bias point solving method was used. It was found that the simulation faced difficulty in solving the initial desired bias points. i.e. ±1V, ±2V, ±3V, ±4V, ±5V, ±6V, ±7V for backgate voltage and ±1V for drain voltage. Therefore, the initial gate bias was set to 0.005V and the next bias point was set to 0.05V, before finally setting the bias point to desired value.

CHEPTER 03: RESULT

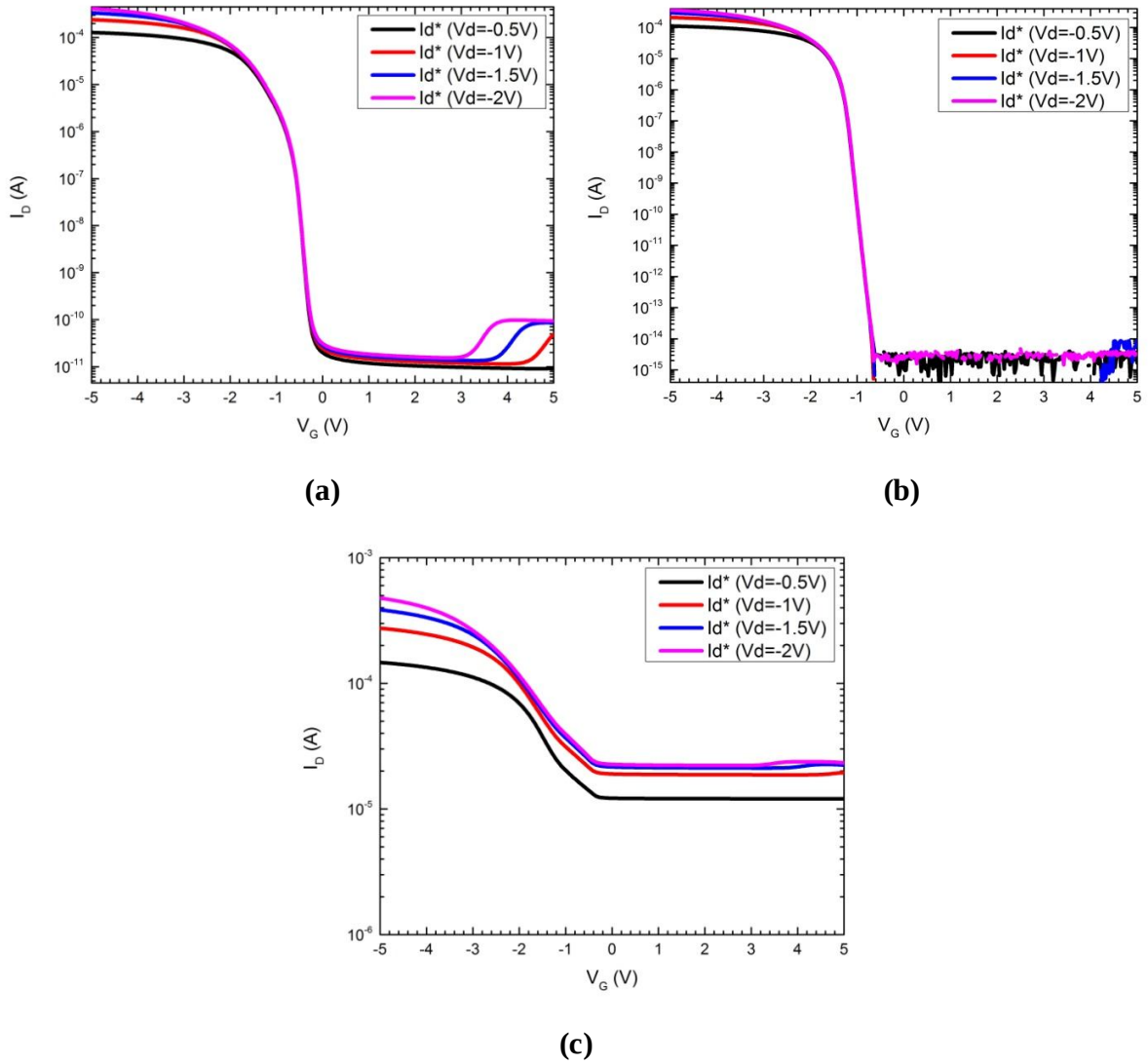

(a) **(b)**

(c)

Figure 3.1: Sub-threshold characteristics of p-type Si NW's at different backgate voltages when NW length is 1um and NW thickness is 100nm. (a) For backgate voltage of 0V. (b) For backgate voltage of +7V. (c) For backgate voltage of -7V. The NW's have a body doping of $10^{17}/cm^3$.

Figure 3.1 (a to c) shows the sub-threshold characteristics (I_D vs V_G) of Si-NW when V_D is negative and V_G is swiped from +5V to -5V at different backgate biases. The nanowire have thickness of 100 nm, doping concentration of 10^{17} $cm^{-3}$and channel length of 1µm.

For 0V backgate bias at Figure 3.1(a) the sub-threshold slope is 114mV/dec. There is no shift of I_D vs V_G curve with increasing V_D values up to -2V indicates that there is DIBL when V_D is negative.

For +7V of backgate bias figure 3.1(b) the sub-threshold characteristics is noticeably improved with a sub-threshold slope of 71.8 mV/dec. There also no shift of I_D vs V_G curve with increasing V_D values up to -2V. Sub-threshold characteristic at this backgate bias is quite good for sensing operation.

For -7Vof backgate bias in figure 3.1(c), the sub-threshold characteristics is reversely degraded and sub-threshold slope is 1742 mV/dec which is not good for sensing operation. This result also show that technical behavior of 1um long and 100 nm thick NW's with a body doping of 10^17/cm^3 can be easily tuned by a backgate arrangement in a 100 nm box standard SOI wafer.

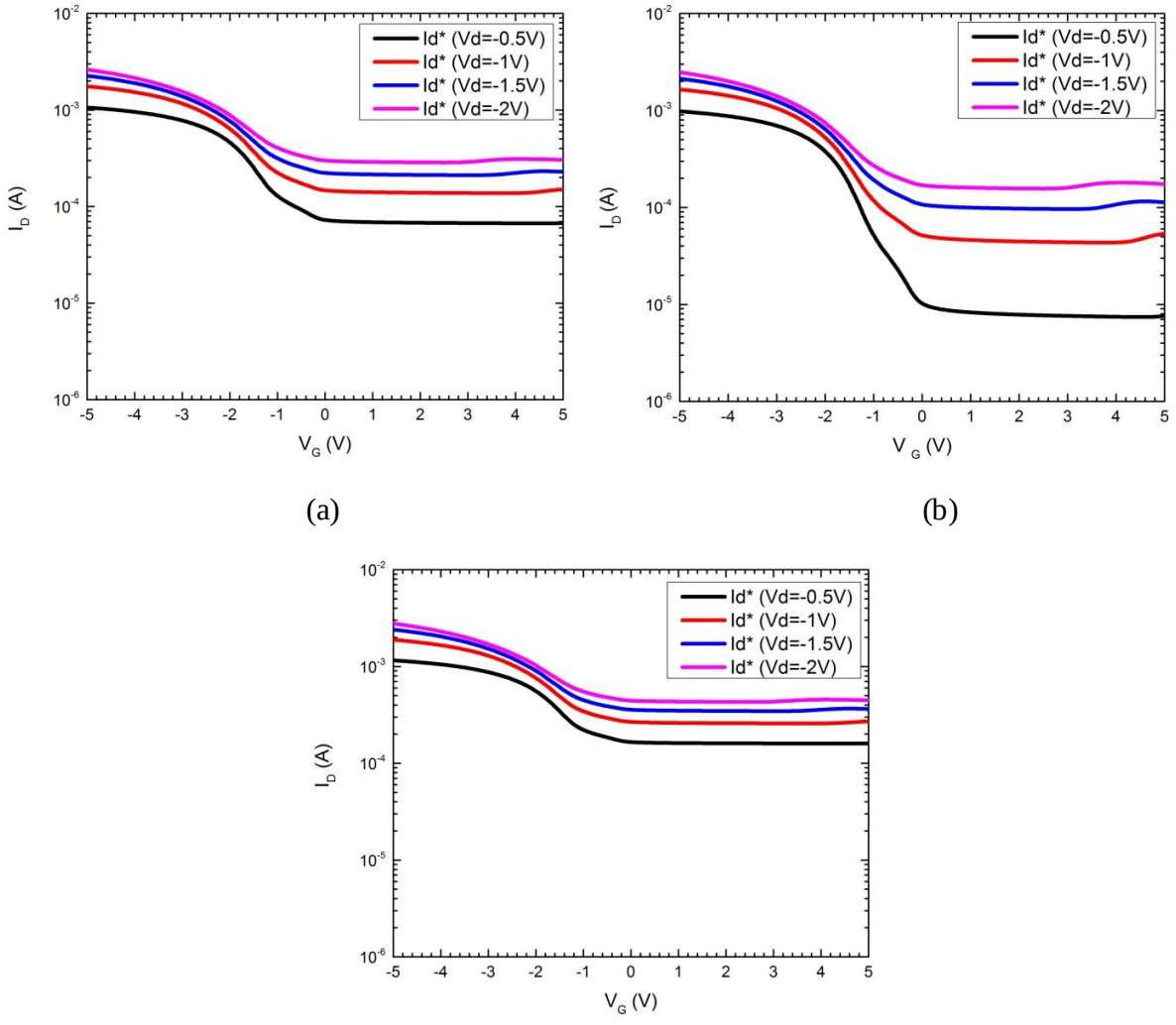

Figure 3.2: Sub-threshold characteristics of p-type Si NW's at different backgate voltages when NW length is 100nm and NW thickness is 100nm. (a) For backgate voltage of 0V. (b) For backgate voltage of +7V. (c) For backgate voltage of -7V. The NW's have a body doping of $10^{17}/cm^3$.

Figure 3.2(a to c) shows transfer characteristics (I_D vs V_G) of Si-NW for 100nm thickness and for 100nm NW length for different values of backgate bias. For 0V of backgate bias, 100 nm long Si-NW shows poor characteristics with a sub-threshold slope of 1667 mV/dec. In addition, DIBL is also evident at 100 nm NW length. This result shows that with the reduction of NW length, sub-threshold characteristic degrades and 100 nm long p-type Si NW with thickness 100 nm is not suitable as a sensor. To investigate the possibility of improving NW characteristic through backgate bias arrangement, figure 3.2(b) shows transfer characteristics of 100 nm NW at +7V of backgate bias. A mild improvement in the sub-threshold characteristics is found with a sub-threshold slope of 1028 mV/dec – which does not look promising as a biosensor. For a backgate bias of -7V in figure 3.2(c), sub-threshold characteristic severely degrades with a slope of 2494 mV/dec. This result shows that a 100 nm long NW with a thickness of 100 nm is not suitable as a biosensor.

Figure 3.3 (a to c) shows the sub-threshold characteristics (I_D vs V_G) of Si-NW when NW thickness is 50nm and NW length is 1um. During this simulation V_D was negative and V_G was swiped from +5V to -5V at different backgate biases.

For a backgate bias of 0V in Figure 3.3(a) the sub-threshold characteristics is better than 100 nm thick Si-NW and sub-threshold slope at this bias voltage is 72.9mV/dec. Again there is no shift of I_D vs V_G curve with increasing V_D values up to -2V. In comparison to 100 nm thick NW, 1 um long Si-NW at 50 nm thickness is better.

For +7V of backgate bias in figure in 3.3(b), the sub-threshold characteristic is much better with a sub-threshold slope of 64 mV/dec. There is also no shift of I_D vs V_G curve with increasing V_D values up to -2V. The value of sub-threshold slope for the 50 nm Si-NW at 1 um channel length is close to the theoretically ideal value of 60 mV/dec and obviously better than the 100 nm thick NW at this backgate bias.

For -7V of backgate bias in figure 3.3(c) show the sub-threshold characteristics is again degraded with a slope value of 1090 mV/dec. Although accumulation of carriers in a p-type Si-NW at 50 nm thickness by the application of -7V backgate voltage degrades sub-threshold behaviour of the NW, it is still better than the 100 nm thick Si-NW (figure 3.2 (c)). The 100 nm thick, 1 um long Si-NW exhibits a sub-threshold slope of 1742 mV/dec. and noticeable DIBL can also be observed. In contrast, the 50 nm Si-NW at this channel length with -7V of backgate bias shows a sub-threshold slope of 1090 mV/dec and there is no significant DIBL as well. This result demonstrates that in general, the 50 nm thick Si-NW exhibits better characteristics in comparison to the 100 nm thick Si-NW

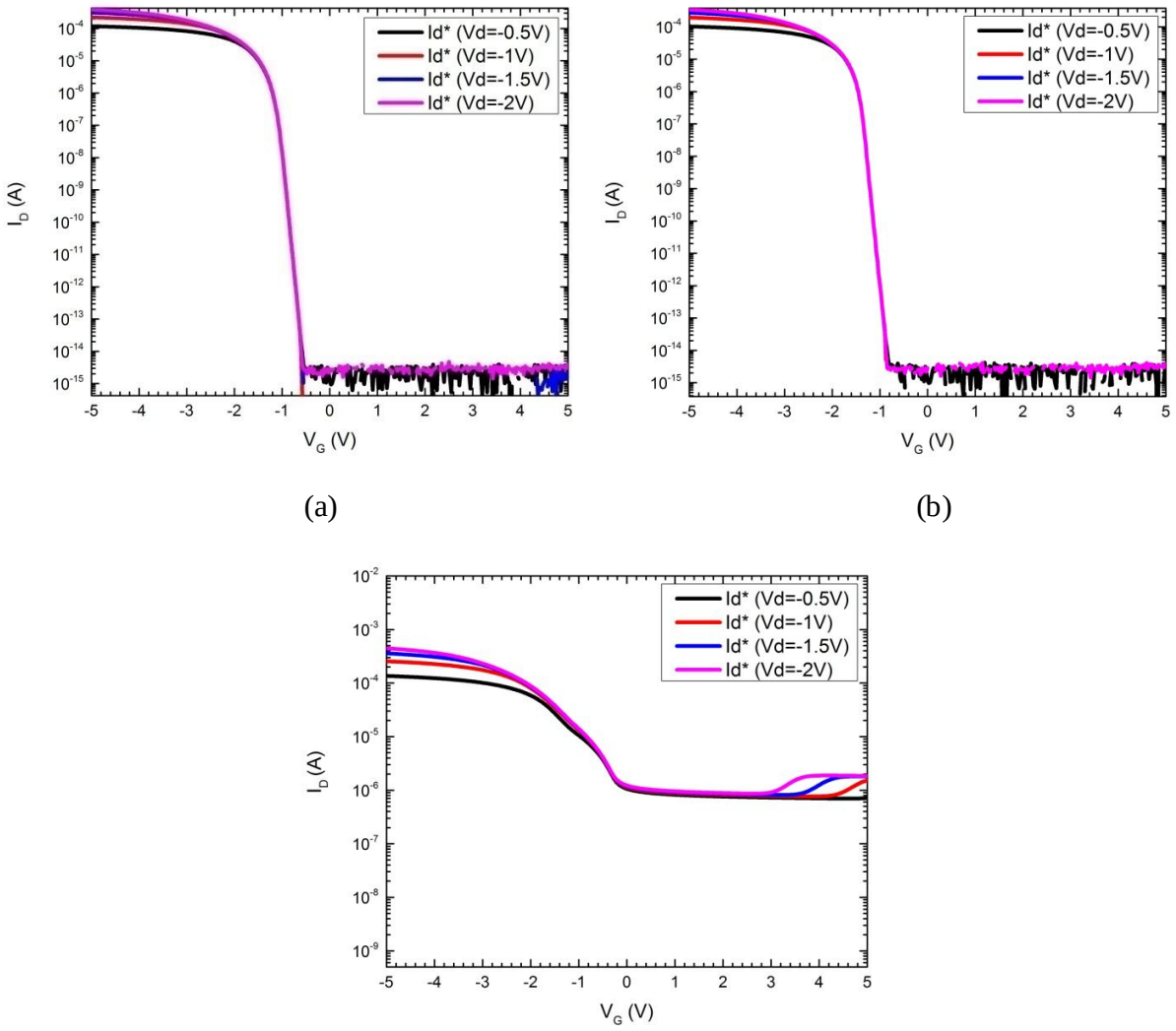

Figure 3.3: Sub-threshold characteristics of p-type Si NW's at different backgate voltages when NW length is 1um and NW thickness is 50nm. (a) For backgate voltage of 0V. (b) For backgate voltage of +7V. (c) For backgate voltage of -7V. The NW's have a body doping of $10^{17}/cm^3$.

To investigate further Figure 3.4 (a-c) shows transfer characteristics of 100 nm long Si-NW when the thickness 50 nm. When the backgate voltage is 0V in figure 3.4(a), the sub-threshold slope has a value of 414.7 mV/dec which is better than the sub-threshold slop of 1667 mV/dec for the 100 nm thick Si-NW at 100 nm length shown in figure 3.2(a). While application of backgate voltage of +7V was able to do minor improvement of the sub-threshold slope to 1028 mV/dec (figure3.2(b)) for 100 nm thick Si-NW, 50 nm Si-NW characteristics has been improved quite a lot upon the application of +7V of backgate bias, (figure 3.4 (b)). The value of the sub-

threshold slope has been improved to 133mV/dec, which is quite promising. The DIBL characteristic is also better than the 100 nm thick NW at this NW length. Wide before application of -7V of backgate bias degrades sub-threshold slope to 2290 mV/dec which is a similar type of degradation found in 100 nm thick Si-NW (figure 3.2 (c)).

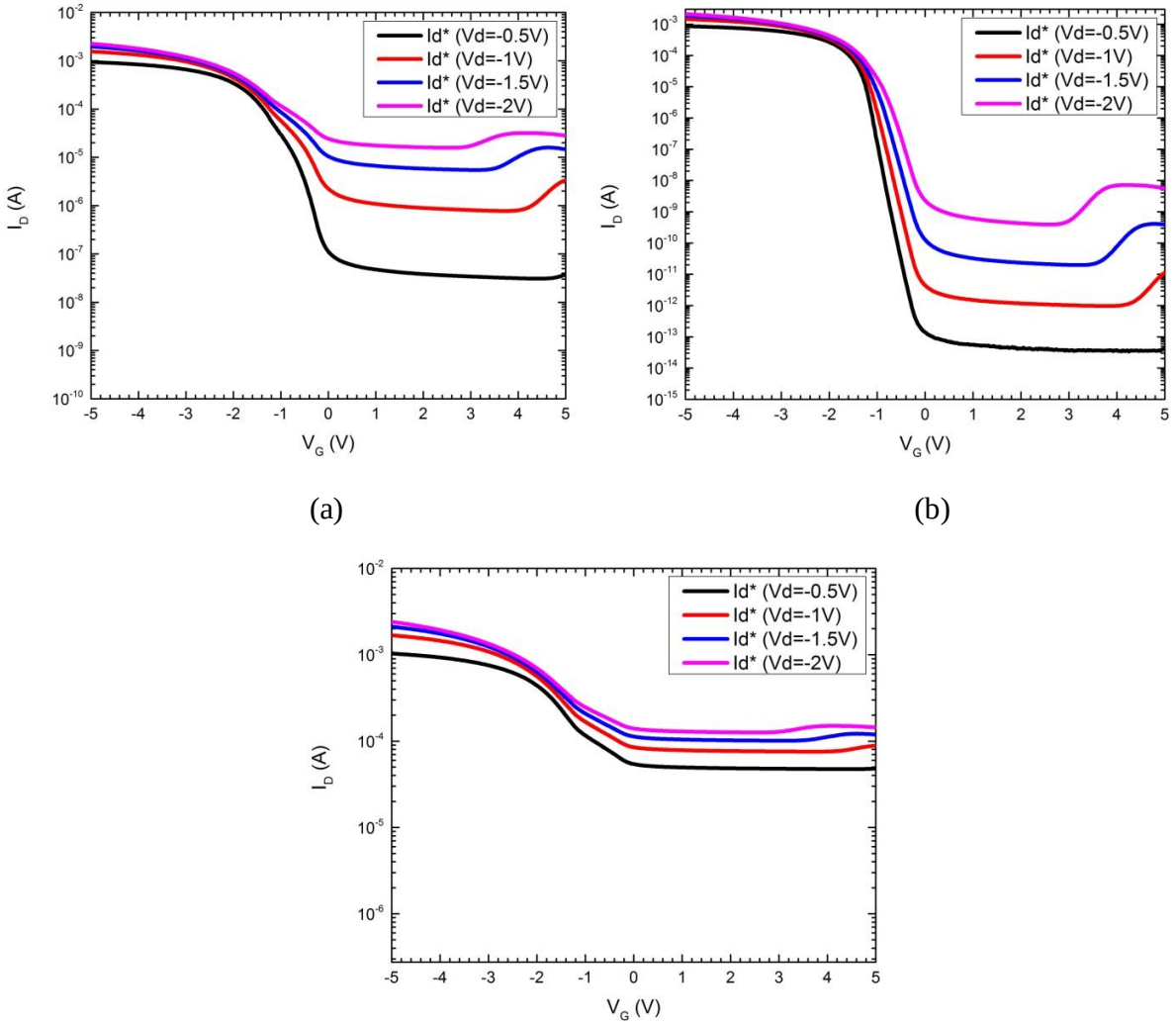

(a) (b)

(c)

Figure 3.4: Sub-threshold characteristics of p-type Si NW's at different backgate voltages when NW length is 100nm and NW thickness is 50nm. (a) For backgate voltage of 0V. (b) For backgate voltage of +7V. (c) For backgate voltage of -7V. The NW's have a body doping of $10^{17}/cm^3$.

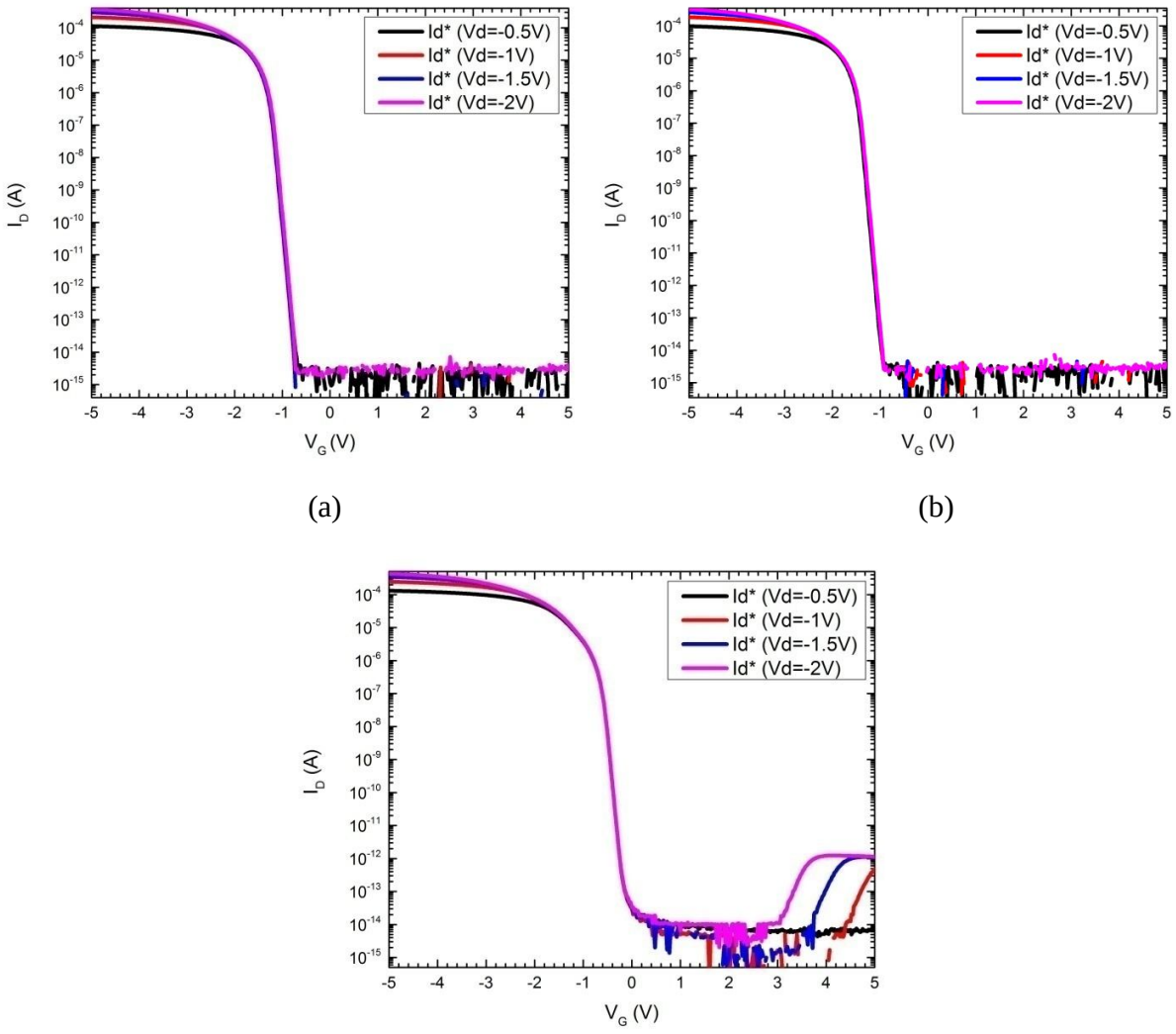

(a) (b)

(c)

Figure 3.5: Sub-threshold characteristics of p-type Si NW's at different backgate voltages when NW length is 1um and NW thickness is 25nm. (a) For backgate voltage of 0V. (b) For backgate voltage of +7V. (c) For backgate voltage of -7V. The NW's have a body doping of $10^{17}/cm^3$.

Figure 3.5 (a to c), it shows that the sub-threshold characteristics of a 25 nm thick NW for 1 um channel length at different backgate biases. At this NW thickness, sub-threshold characteristic seems to be quite robust which is not affected too much for different values of backgate biases.

Here the sub-threshold slopes are 65.5 mV/dec , 61 mV/dec , 72.1 mV/dec at backgate bias 0V , +7V and -7V respectively. Furthermore, there are no shifts in the I_D vs V_G curves with V_D values up to -2V at all three backgate bias voltages. These results show that 25 nm thick Si-NW is quite promising as a sensor at 1um channel length.

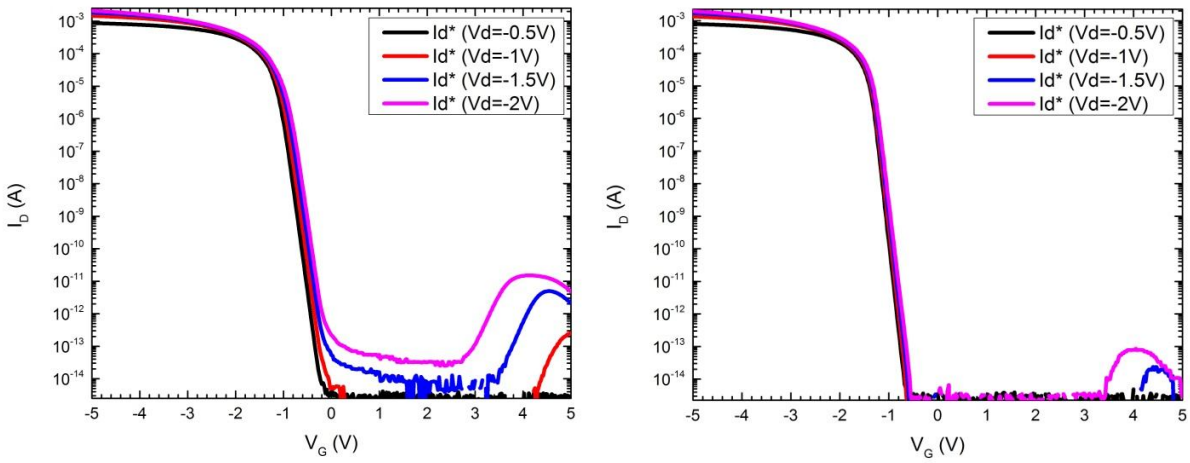

(a) (b)

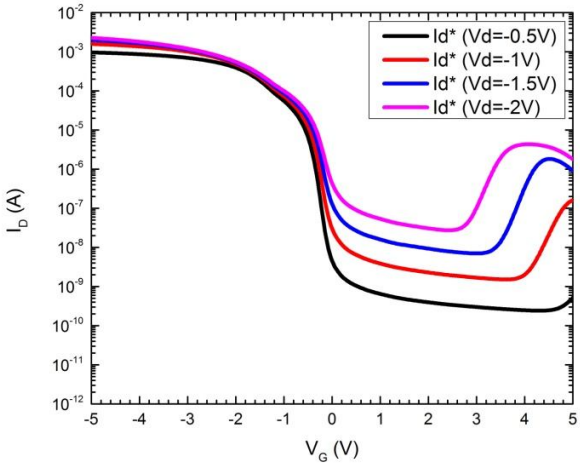

(c)

Figure 3.6: Sub-threshold characteristics of p-type Si NW's at different backgate voltages when NW length is 100nm and NW thickness is 25nm. (a) For backgate voltage of 0V. (b) For backgate voltage of +7V. (c) For backgate voltage of -7V. The NW's have a body doping of $10^{17}/cm^3$.

Figure 3.6 (a-c) shows electrical characteristics of 25 nm thick Si-NW for the shortest NW length of 100 nm. It is observed that 100 nm long and 25 nm thick Si-NW characteristics are much better than the 100 nm and 50 nm NW thickness at all backgate biases.

Here the sub-threshold slopes are 94.4mV/dec, 73.6mV/dec, and 124.9mV/dec at backgate bias 0V, + 7V and -7V respectively. There are no shifts of I_D vs V_G curves with V_D values up to -2V at all three backgate bias voltages.

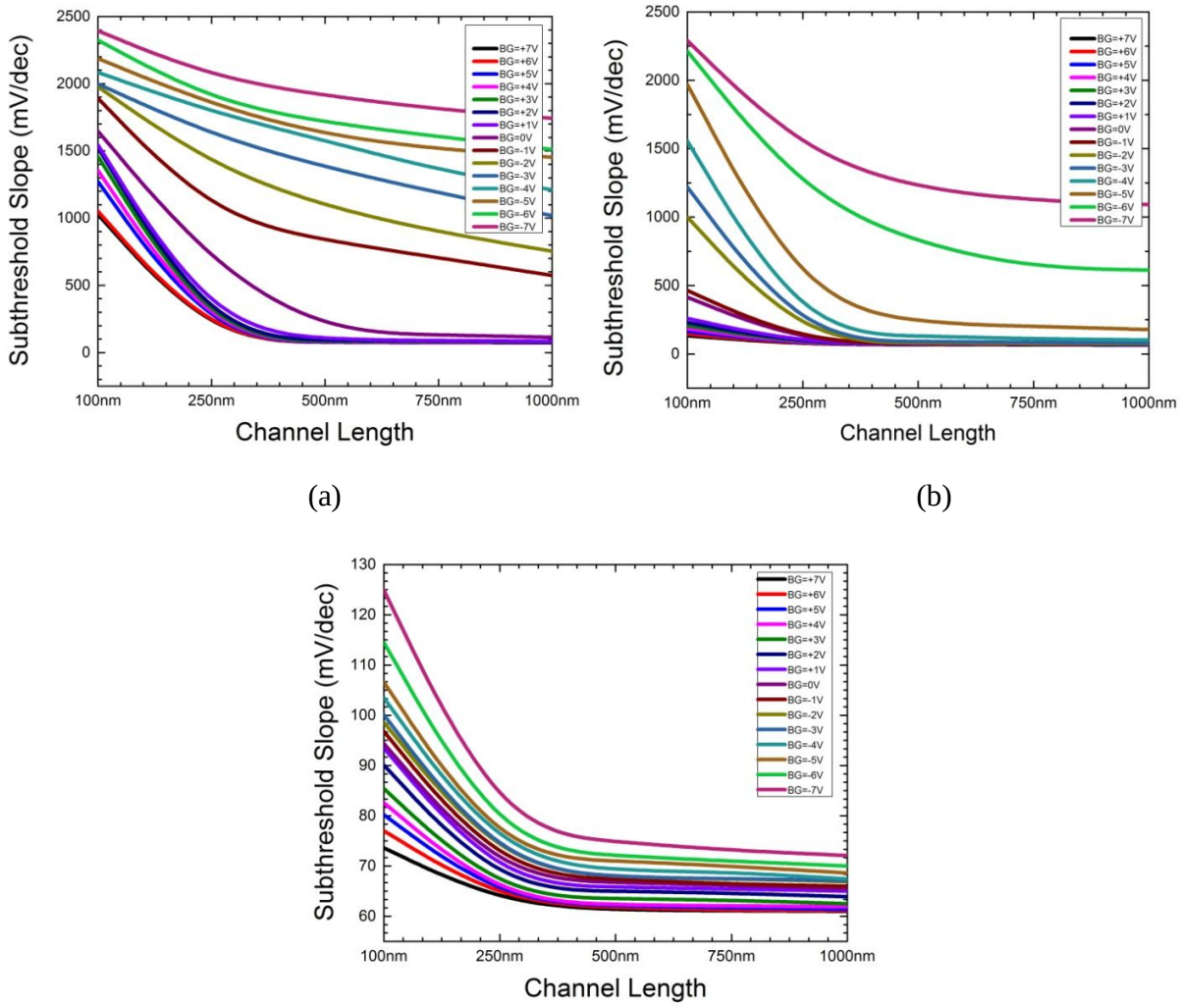

Figure 3.7: Sub-threshold slope as a function of channel length for different backgate biases and for different NW thickness (a) NW thickness of 100nm (b) NW thickness of 50nm (c) NW thickness of 25nm

Figure 3.7 (a to c) summarizes sub-threshold slopes of Si-NWs at different thicknesses and at different NW lengths. For 100 nm Si thickness, best values of sub-threshold slopes are obtained when significant depletion is created by +7V of backgate biased. In figure 3.7(a) the calculated value of sub-threshold slope at +7V of backgate bias are 71.8mV/dec for 1 um long channel length. This value is approximately maintained up to 350 nm of NW length. However, at beyond 350 nm length device degrades and sub-threshold slope becomes 1028mV/dec at 100 nm NW length. When backgate bias is decreased from +7V to -7V, the device degrades gradually.

For -7V of backgate bias, the sub-threshold slope is 1742 mV/dec for 1um NW length whereas 2394mV/dec for 100 nm NW length.

A similar characteristic is observed for 50 nm NW length as shown in figure 3.7 (b) but the sub-threshold slope values are significantly better than the 100 nm thick Si-NW. The best characteristics are obtained from the 25 nm NW thickness (figure 3.7(c)) where even the 100 nm Si-NW also exhibits good sub-threshold characteristics. At +7V of backgate bias, the 100 nm long 25 nm thick NW exhibits a sub-threshold slope of 73.6 mV/dec which is merely degrades to a value of 124.9 mV/dec at -7V of backgate bias.

Figure 3.8 shows the extracted values of sensitivity of 1 um long p-type Si-NW with 100 nm thickness for different backgate biases. The results are shown for different values of negative V_D values. The gate sensitivity is calculated using a simple one-dimensional relationship of following equation using data from the sub-threshold slope.

$$\text{Sensitivity} = \frac{(I2 - I1)}{(I2 * (VG2 - VG1))} * 100\ (\%/V) \tag{4.1}$$

During this calculation only linear and saturation region of sub-threshold characteristics are considered and off-state of NW is avoided. For 0V of backgate bias in figure 3.8(a), it is found that the peak sensitivity is around 1930 %/V for V_D = -0.5V at V_G= -0.45V which reduces to a value of 7.62%/V at V_G= -5V. For V_D = -1V the peak sensitivity is 1920%/V at V_G= -0.45V which again reduces to a value of 9.23 %/V at V_G= -5V.

Similar trend is continued for V_D = -1.5V and -2 V. The peak sensitivity corresponds to the linear region of sub-threshold plot shown in figure 3.1(a) and hence, some sensitivity is observed as the sub-threshold characteristic is overlapping in figure 3.1(a) at these V_G values. However in the saturation region of figure 3.1(a), the rate of change of I_D with V_G is increasing with increasing V_D values and therefore, sensitivity is increasing with increasing negative values of V_D. In saturation region of V_G = -5V, a similar trend is found for backgate voltage of +7V and -7V.

In figure 3.8(b) and 3.8(c) however at a backgate bias of +7V the peak sensitivity is 2220 %/V at V_G = -1.08V and at -7V of backgate bias, the peak sensitivity is significantly reduced to a value of 144%/V. The peak sensitivity values, corresponding V_G and $V_{backgate}$ values are pretty important for the application of NWs as sensors. It provides the necessary values of liquid gate and backgate voltages for obtaining maximum sensitivity of NWs for a particular dimension.

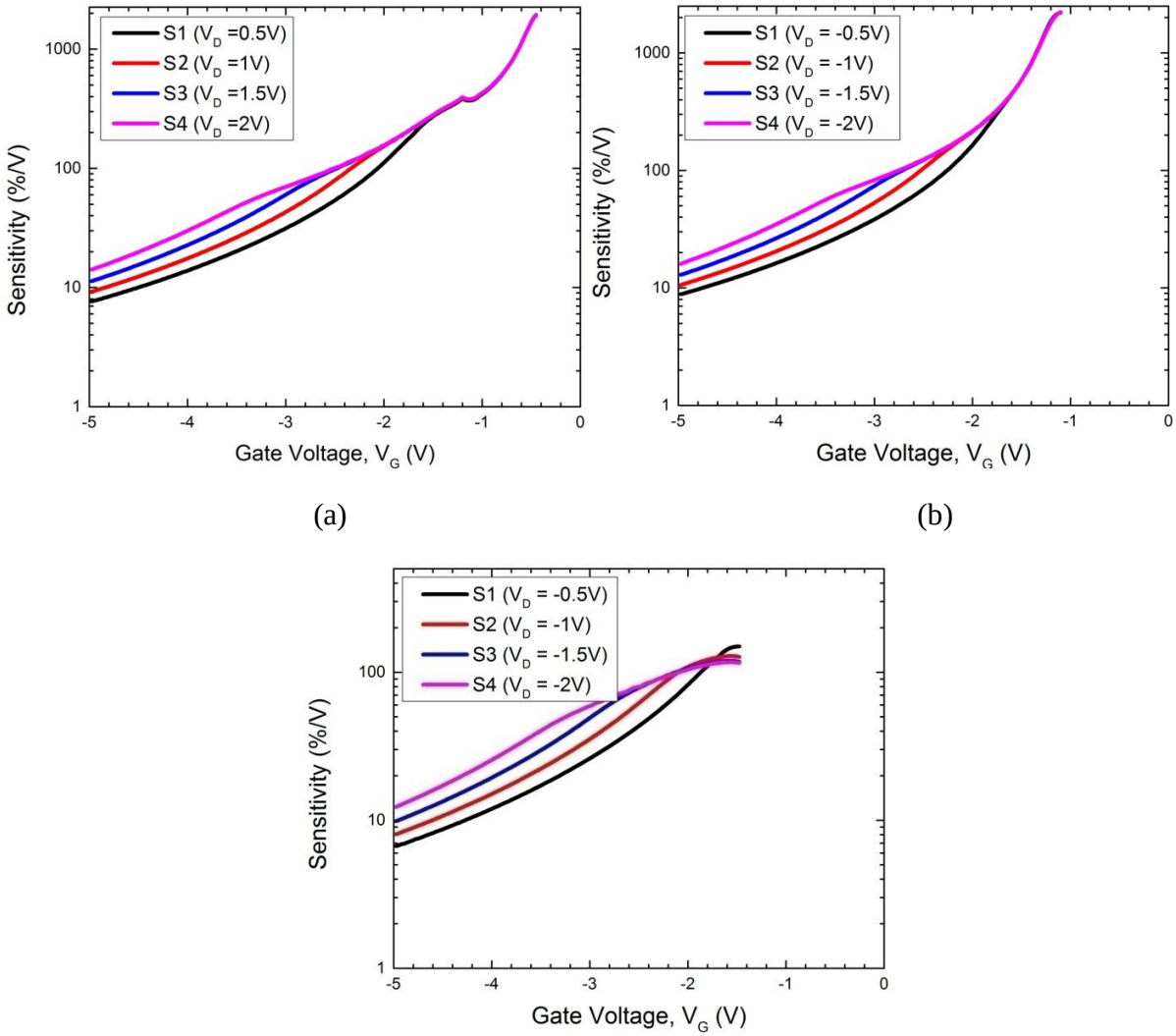

Figure 3.8: Sensitivity (%/V) of p-type Si NW's at different backgate voltages when NW length is 1000nm and NW thickness is 100nm. (a) For backgate voltage of 0V. (b) For backgate voltage of +7V. (c) For backgate voltage of -7V. The NW's have a body doping of $10^{17}/cm^3$.

The extracted values of peak sensitivity may be the targeted point of NW as a sensor. Hence in figure 3.9 (a to c) shows sensitivity as a function of NW lengths for three different NW thicknesses. The results are plotted for different backgate biases. For 100 nm thick Si NW, In figure 3.9(a) the maximum sensitivity 2390%/V can be achieved for 1 um long NW and that is maintained down to 350 nm NW length. Beyond 350 nm, sensitivity reduces and at 100 nm NW length, maximum achievable sensitivity is 349%/V.

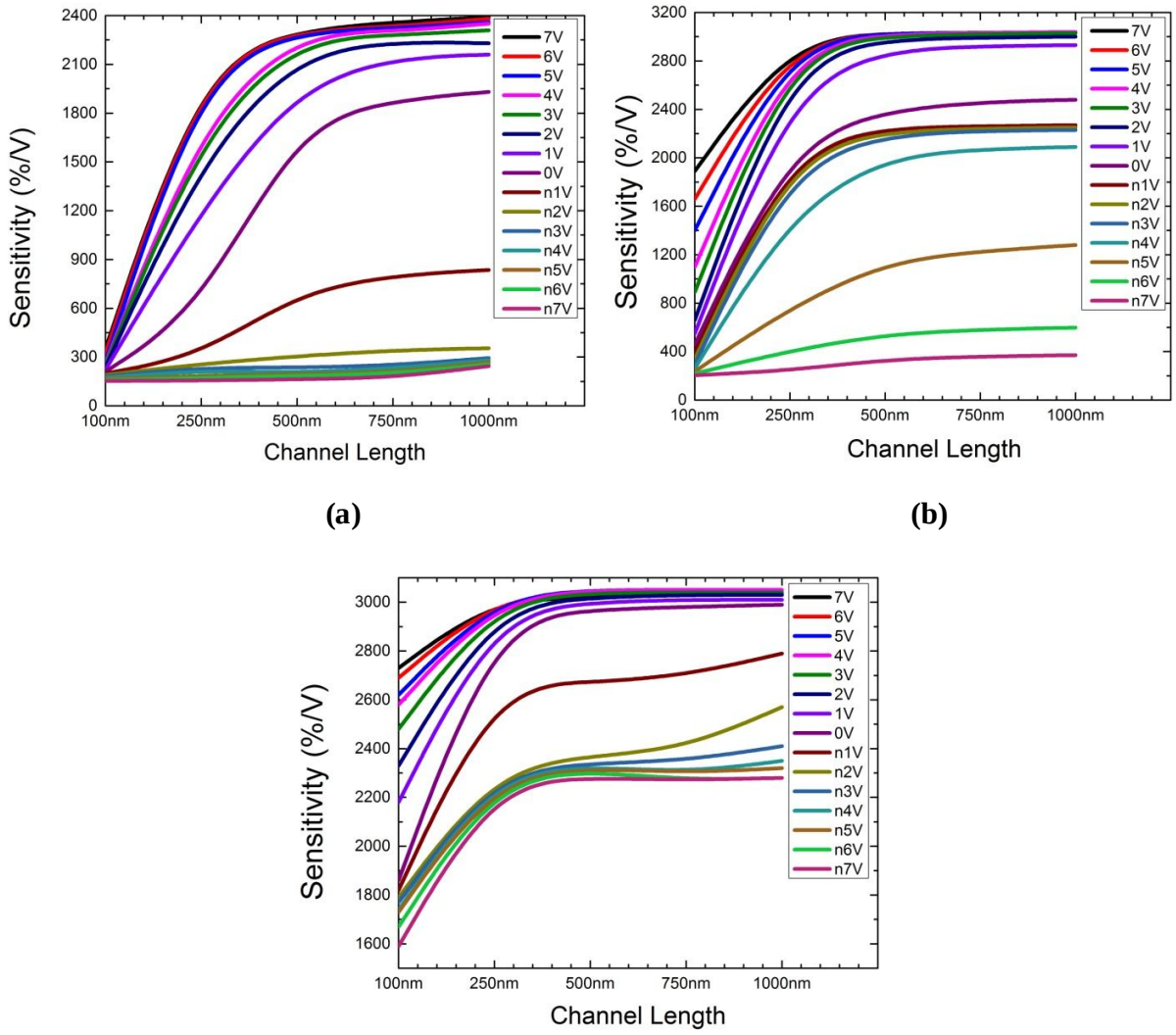

Figure 3.9: Sensitivity as a function of channel length for different backgate biases and for different NW thickness (a) NWs thickness of 100nm (b) NW thickness of 50nm (c) NW thickness of 25nm

With decreasing backgate bias voltages, this sensitivity reduces. For -7V of backgate voltage 1um long NW exhibits sensitivity of 244%/V and at 100 nm NW length it is 152%/V showing that the NW length is independent of sensitivity due to too much carrier accumulation. Similar trend is found for 50 nm and 25 nm Si-NWs in figure 3.9 (b and c).

However it can be easily observed that with the decrease of NW thickness, maximum achievable sensitivity increases for all NW lengths and for 25 nm thick NWs even 100 nm NWs can be used as sensors.

CHAPTER 04: CONCLUSION

We performed a feasibility study of tailoring sensitivity of Si nanowire through backgate bias arrangement for various NW length and thickness. Three different thicknesses of 100 nm, 50 nm and 25 nm were chosen and each thickness consisted of 5 different channel lengths - 1000 nm, 750 nm, 500 nm, 250 nm and 100 nm respectively. It can be seen that the backgate bias has a big influence on the sensitivity of a p-type SiNW. A backgate bias leading to a depletion of the NW body increases the sensitivity whereas the backgate bias leading to an accumulation of significant carriers decreases the sensitivity of NW. For a fixed NW thickness, a decrease of NW length found to degrade sub-threshold slope and hence NW sensitivity. But for a fixed NW length a decrease of NW thickness improves the sub-threshold characteristics and sensitivity. When the NW thickness is 100 nm a peak sensitivity of 2390%/v is found for 1um long NW which degrades to a value of 349%/V at 100nm length. However, 100 nm long NW's sensitivity can be improved by reducing NW thickness and adjusting backgate bias. A 100 nm long 25 nm thick NW exhibits an improved sensitivity of 2730%/V with +7V of backgate bias. This result implies that with appropriate backgate bias arrangement, low doped then NW can be used for single molecule detection as biosensors. Our simulation revealed that a 25 nm thick 1 um long NW with +7V of backgate bias gives a sensitivity of 3050 %/V.

References

[1] Y. Chen, X. Wang, M. K. Hong, S. Erramilli, P. Mohanty and C. Rosenberg," Nanoscale Field Effect Transistors for Biomolecular Signal Amplification", Appl. Phys., let. 91, pp. 243511, 2007.

[2] Cui, Y., and Lieber, C. M., "Nanowire and Nano sensor for highly sensitive and selective detection of biological and Chemical species", Science, vol.293, pp 1289-1292

[3] Songyue Chen, Johan G. Bomer, Wilfred G. van der Wiel, Edwin T. Carlen, and Albert van den Breg, "Top-Down Fabrication of Sub-30nm Monocrystalline Silicon Nanowires Using Conventional Microfabrication", American Chemical society ^{ACS} NANO, vol.3,No.11,pp. 3487-3490,2009.

[4] J. Colinge, C. Lee, A. Afzalian, A. Dehdashti, 1. Yan R. Ferain, P. Razavi, B. O'Neil, A. Blake, M. White, A. Kelleher, B. McCarthy, and R. Murphy, "Nanowire transistors without junctions," Nature Nanotecnology, vol.5,pp. 225-229,2010.

[5] Zhiyong Zhang, Kun Yao, Yang Liu, Chuanhong Jin, Xuelei Liang, Quing Chen, and Lian-Mao Peng, "Quantitative Analysis of Current-Voltage Characteristics of semiconducting Nanowires: Decoupling of Contact effects",Wiley Inter Science,pp. 387-392, 2007.

[6] Y. Bunimovich, Y. Shin, W. Yeo, M. Amori, G. Kwong, and J. Heath, "Quantitative real time measurements of DNA hybridization with alkylated nanoxidized silicon nanowires in electrolyte solution," J. Am. Chern. Soc., vol. 128, pp. 16323-16331, Dec. 2006.

[7] Y. Wu, P. Hsu, and W. Liu, "Polysilicon wire for the detection of level free DNA," Journal of The Electrochemical Society, vol. 159, no. 6, pp.J191-J195, 2010.

[8] J. H. Chua, R.E. Chee, A. Agarwal, S.M. Wong, and G. Zhang, "Label-free electrical detection of cardiac biomarker with complementary metal-oxide semiconductor compatible silicon nanowire sensor arrays," Analytical Chemistry, vol. 81, no. 15, pp. 6266-6271, 2009.

[9] N.Elfstrom, A. Karstrom, and J. Linnors, "Silicon nanoribbons for electrical detection of biomolicules," Nano Letters, vol. 8, pp. 945-949, 2008.

[10] A. Cattani-Scholz, D.Pedone, M. Dubey, S. Peppi, S. Nickel, P. Feulner, J. Schwartz, G. Abstrelter, and M. Tornow," Organophosphonate-based pnafunctionalization of silicon nanowires for level free DNA detection," ACS NANO, vol. 2, no. 8, pp. 1653-1660, 2008.

[11] A. Agarwal, I. Lao, K. Buddharaju, N. Singh, N. Balasubramanian, and D. Kwong, "Silicon nanowire array bio-sensor using top-down CMOS technology," Solid-State sensors, Actuatorsand Microsystems Conference, 2007. TRANSDUCERS 2007, International, pp. 1051-1054, 10-14, June 2007.

[12] P.Hsu, J. Lin, W. Hung, and A.cullis, “Ultra-sensitive polysilicon wire glucose sensornusing a 3-aminopropyltriethoxysilane and polydimethylsiloxne-treated hydrophobic fumed silica particle mixure as the sensing membrane,” Sensors and Actuators B: Chemical, pp. 273-279, 2009.

[13] Mohammad M. A.Hakim, M.Lombardini, K.Sun, F.Giustiniano, P.L.Roach, D.E. Davies, P.H.Howarth, M. R. R.de Planque, H. Morgan, P. Ashburn, “Thin film polycrystalline silicon nanowire biosensors,” Nano Letters, vol. 12, Issue 4, pp. 1868-1872, 2012.

[14] Atlas user’s Manual: Device Simulation Software, 2008.

[15] C. J. Su, T. I Tasi, Y. L.Liou, Z. M Lin, H. C.Lin, and T.S. Chao, “Gate-All-Around Junctionless Transistors With Heavily Doped Polysilicon Nanowire Channels,” IEEE Electron Device Letters, vol. 32, no. 4, pp. 521-523, Apr.2011.